Calculation and Measurement of Electromechanical Coupling Coefficient of Capacitive Micromachined Ultrasonic Transducers

Goksen G. Yaralioglu, *Member, IEEE*, Arif Sanli Ergun, *Member, IEEE*, Baris Bayram, Edward Hæggström, and Butrus T. Khuri-Yakub, *Fellow, IEEE*

***Abstract*—The electromechanical coupling coefficient is an important figure of merit of ultrasonic transducers. The transducer bandwidth is determined by the electromechanical coupling efficiency. The coupling coefficient is, by definition, the ratio of delivered mechanical energy to the stored total energy in the transducer. In this paper, we present the calculation and measurement of coupling coefficient for capacitive micromachined ultrasonic transducers (CMUTs). The finite element method (FEM) is used for our calculations, and the FEM results are compared with the analytical results obtained with parallel plate approximation. The effect of series and parallel capacitances in the CMUT also is investigated. The FEM calculations of the CMUT indicate that the electromechanical coupling coefficient is independent of any series capacitance that may exist in the structure. The series capacitance, however, alters the collapse voltage of the membrane. The parallel parasitic capacitance that may exist in a CMUT or is external to the transducer reduces the coupling coefficient at a given bias voltage. At the collapse, regardless of the parasitics, the coupling coefficient reaches unity. Our experimental measurements confirm a coupling coefficient of 0.85 before collapse, and measurements are in agreement with theory.**

I. Introduction

CAPACITIVE micromachined ultrasound transducers (CMUTs) have been demonstrated to work efficiently for both air and immersion applications [1]–[3]. A CMUT consists of many metalized membranes supported above a bottom electrode. The metalization on the membrane forms the top electrode. When an alternating current (AC) voltage is added to a direct current (DC) bias voltage that applied between the electrodes, a sinusoidal membrane vibration is obtained. If the biased membrane is exposed to an incoming acoustic field, electrical current is delivered to an external load. Basically, the CMUT converts electrical energy into mechanical energy and vice versa. When operating with an electrical input, the electromechanical conversion or coupling coefficient k relates the amount of mechanical energy delivered to the load to the total energy stored in the device:

$$k_T^2 = \frac{E_{\text{mech}}}{E_{\text{total}}} = \frac{1}{1 + \frac{E_{\text{elec}}}{E_{\text{mech}}}}, \tag{1}$$

where $E_{\text{total}} = E_{\text{elec}} + E_{\text{mech}}$. Traditionally, the subscript T is often used to define the conversion efficiency for piezoelectric transducers clamped in the direction transverse to the electric field [4, p. 33]. The transducer motion is parallel to the field. This is also the case for CMUTs because the membrane moves in the direction of the applied electric field, and the membrane motion in the transverse direction is minimal. Therefore, throughout the text, k_T^2 is used to denote the coupling coefficient for CMUTs.

The coupling coefficient is an important parameter because it characterizes the transducer. For piezoelectric transducers, the transducer bandwidth, for example, is determined by k^2 [4, p. 59]. Thus, the evaluation of this parameter has attracted the attention of many researchers.

Hunt [5, p. 181] calculated k_T^2 for condenser microphones in which the device is modeled by a parallel plate capacitor with a moving top electrode. In this model, a spring supports the top electrode and the bottom plate is fixed. A bias voltage is applied to the top plate; the bottom plate is kept at zero potential. Under the applied bias voltage, the top plate is attracted toward the bottom plate. This approach neglects the deformation of the membrane supported at its rim and assumes the membrane is moving like a piston. Senturia [6, p. 172] also calculated coupling coefficient by deriving small signal two-port representation for the parallel plate capacitor. For the parallel plate structure, the coupling coefficient is:

$$k_T^2 = \frac{2x}{d_0 - x}, \tag{2}$$

where d_0 is the initial gap distance between the plates when the bias voltage is zero, and x is the top plate displacement due to the applied bias. Initially, k_T^2 is zero and increases as the displacement increases. When the displacement equals to one-third of the initial gap distance,

Manuscript received July 30, 2002; accepted January 7, 2002. This work is supported by the Office of Naval Research. Dr. Hæggström acknowledges the financial support of the Wihuri Foundation and the academy of Finland.

G. G. Yaralioglu, A. S. Ergun, B. Bayram, and B. T. Khuri-Yakub are with E. L. Ginzton Laboratory, Stanford University, Stanford, CA 94305 (e-mail: goksenin@stanford.edu).

E. Hæggström is a visiting scholar at E. L. Ginzton Laboratory, on leave from the Department of Physics, University of Helsinki, Helsinki, FIN-00014, Finland.

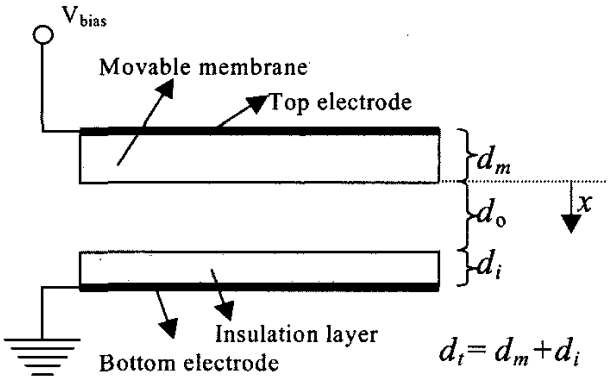

Fig. 1. Parallel plate transducer. The effective dielectric constant of the insulation layer and the membrane material is ε_r, d_m is the membrane thickness, d_i is the insulator layer thickness, and d_0 is the gap distance under zero bias.

the electrostatic force gradient is larger than that of mechanical force and the top plate collapses on the bottom electrode; at this point k_T^2 is equal to 1 [5, p. 186]. Later, Eccardt *et al.* [7] calculated the coupling coefficient and investigated the effect of parallel parasitic capacitance for CMUTs using the parallel plate approximation. However, Eccardt's analysis neglects the spring softening effect [5, p. 181], [6, p. 168]. Due to the electrical field applied on the membrane, the apparent small signal spring constant is lowered by the electromechanical interaction. The softened spring constant is given by [6, p. 134]:

$$k_s' = k_s - \frac{A\varepsilon_0 V^2}{(d_0 - x)^3}, \tag{3}$$

where k_s is the spring constant of the membrane. Detailed derivation for the spring softening is given in the Appendix. If the above change (3) is made in the analysis of [7], one obtains the same result as in (2) for parallel plate capacitors.

In the above analyses, the membrane is assumed to be conducting and the gap is formed between two conductors. However, the CMUT membrane usually is made of a dielectric material, and the electrode is placed on top of the membrane. In addition, there is a thin insulation layer covering the bottom electrode. Consequently, the gap is formed between the bottom of the membrane and the top surface of the insulation layer. The membrane and the insulation layer make up a capacitor in series with the gap capacitance as shown in Fig. 1. The series capacitance is independent of the membrane motion; it does not change as opposed to the gap capacitance. The effect of the series capacitance can be included in the above analysis by defining an effective gap distance:

$$d_{\text{eff}} = d_0 + \frac{d_i}{\varepsilon_r}, \tag{4}$$

where d_t is the total thickness of the dielectric material of which the membrane and the insulation layer is made, and ε_r is the relative dielectric coefficient of the material. The series capacitance increases the collapse voltage and the membrane displacement at collapse. Derivations for the collapse voltage are given in the Appendix. If there is a series capacitance to the gap capacitance, collapse occurs when the membrane displacement is equal to one-third of the effective gap height which is defined in (4). Therefore, if the thickness (d_t) corresponding to the series capacitance is chosen too large such that:

$$\frac{d_t}{\varepsilon_r} > 2d_0, \tag{5}$$

the capacitor may never go into collapse as the membrane will simply touch the substrate at high voltage, and the maximum achievable k_T^2 will be less than 1 for the structure. Hence, it is possible to fabricate devices that do not collapse but that still poses a k_T^2 value close to 1 by carefully adjusting the series capacitance. As will be shown later, these results also apply to membranes supported at their edges. Addition of a series capacitance also has been studied in the literature for electrostatic actuators [8]. The negative feedback provided by the series capacitance stabilizes the actuator and enables the moving electrode to achieve a larger displacement beyond the collapse limit.

Recently, Fraser *et al.* [9] calculated k_T^2 for a CMUT membrane using a derivation based on Berlincourt [10, p. 69] that relies on the use of the fixed (C^S) and free (C^T) capacitance of the transducer. This derivation uses charge and voltage rather than electrical displacement and electric field as in [10]. The resulting coupling coefficient agrees with the Hunt's [5] and Senturia's [6] calculations for parallel plate capacitors. The fixed capacitance is defined as the total capacitance of the transducer at a given DC bias:

$$C^S = \left.\frac{Q(x)}{V}\right|_{x_{\text{DC}},V_{\text{DC}}} = \left.C(x)\right|_{x_{\text{DC}},V_{\text{DC}}}. \tag{6}$$

The free capacitance is defined as the slope of the charge-voltage curve:

$$C^T = \left.\frac{\mathrm{d}Q(x)}{\mathrm{d}V}\right|_{x_{\text{DC}},V_{\text{DC}}} = \left.\frac{\mathrm{d}}{\mathrm{d}V}\left(VC^S\right)\right|_{x_{\text{DC}},V_{\text{DC}}}, \tag{7}$$

and the coupling coefficient is given by:

$$k_T^2 = 1 - \frac{C^S}{C^T}. \tag{8}$$

In this paper, we use Berlincourt's [10] approach to calculate the coupling coefficient. First, the validity of the finite element method (FEM) modeling is tested using the known parallel plate transducer solution for k_T^2. Next, the FEM model is used to calculate the electromechanical coupling coefficient of the CMUT and the influence of parasitic capacitances on this coefficient. In the experimental part, theoretical results are compared to measurements of the coupling coefficient; and it will be shown that the measured k_T^2 values agree with the theoretical prediction of the coupling coefficient.

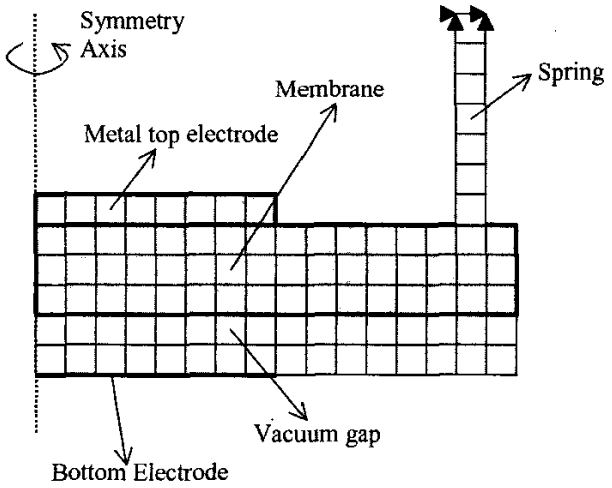

Fig. 2. Finite element mesh used for the modeling of parallel plate capacitor.

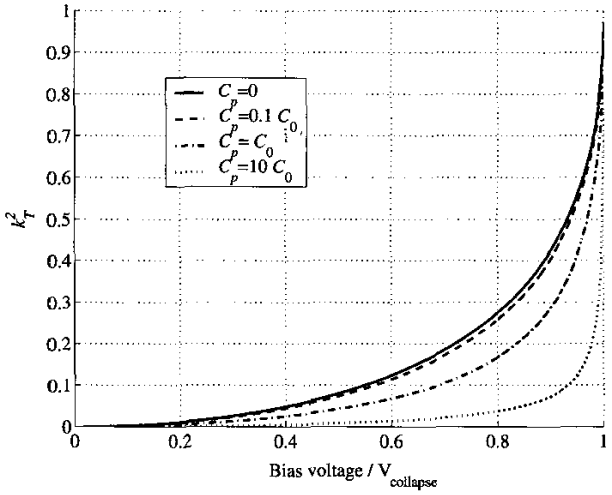

Fig. 3. Calculated coupling efficiency for parallel plate capacitor. C_p is the parallel parasitic capacitance, C_0 is the device capacitance under zero DC bias.

II. FEM Calculations

We tested FEM calculations on the simple model for the parallel plate capacitor depicted in Fig. 1. A commercially available software package, ANSYS 5.7 (ANSYS Inc., Canonsburg, PA), is used for the modeling. A sketch of the FEM model is shown in Fig. 2. Planar elements (PLANE121, PLANE82) are used for the finite element mesh. Because the geometry is symmetric around a line passing through the center of the membrane, an axi-symmetric model is assumed. The moving electrode is attached to the one end of a soft spring. The other end of the spring is restricted from movement. The stiffness of the moving electrode is set to be orders of magnitude larger than the spring constant of the spring. Consequently, the bending of the electrode can be ignored, and the electrode is assumed to be moving like a rigid piston under the applied voltage between the electrodes. First, electrostatic analysis is performed to find the electrostatic forces on the membrane. Then, the displacement of the membrane due to the electrostatic forces is calculated by performing a structural static analysis. New displacement of the membrane is used to find the modified electrostatic forces. These steps are iterated until an equilibrium membrane displacement is reached. At the equilibrium position, the capacitance of the CMUT is extracted using electrostatic analysis. This capacitance is later used to calculate the free capacitance and the coupling coefficient through (7) and (8), respectively.

The calculated k_T^2 is depicted in Fig. 3 for different parallel parasitic capacitance values. The solid curve (no parasitic case) in Fig. 3 is the same as the curve defined by (2). To demonstrate the effect of parallel parasitics, we assumed an external parallel capacitance, C_p, to the actual device capacitance at a given bias voltage. In Fig. 3, C_0 is equal to the capacitance of the device when there is no applied bias. As the parasitic capacitance increases, the k_T^2 curve becomes steeper close to collapse. For each parasitic capacitance value, the electrode is placed on top and on the bottom of the membrane. This changes the series capacitance. In both cases, identical curves are obtained when the bias voltage is normalized with respect to collapse voltage. Therefore, the coupling coefficient appears to be independent of the location of the electrode in the vertical direction inside the membrane. The electrode location (or the series capacitance) changes the collapse voltage. In addition, at the collapse, the maximum membrane displacement increases as the series capacitance increases.

In summary, our FEM calculations for the parallel plate capacitor matched with (2) and thus verified our FEM model. It also showed that, regardless of the parallel parasitic capacitance, the coupling coefficient always goes to unity. Parallel parasitics affect the shape of the k_T^2 curve in such a way that, for a given normalized bias voltage, the coupling efficiency decreases as the parallel parasitics increase.

For the calculation of k_T^2 of an actual CMUT membrane, the model depicted in Fig. 4 is used. The membrane is supported at its rim as shown in Fig. 4. Therefore, this model includes the bending of the membrane. For this structure, the coupling coefficient is calculated for various electrode sizes. The results are shown in Fig. 5. When the electrode radius is less than half of the membrane radius, the coupling coefficient as a function of normalized bias voltage does not change significantly with the changing electrode size. As the electrode radius increases beyond one-half of the membrane radius, the coupling coefficient curve shifts down as shown in Fig. 5. But at the collapse, it still goes to unity. Increasing the electrode radius increases the device capacitance or fixed capacitance. But the increase in the free capacitance is relatively slow compared to that of fixed capacitance. This is due to the fact that most of the membrane deflection is concentrated around the mem-

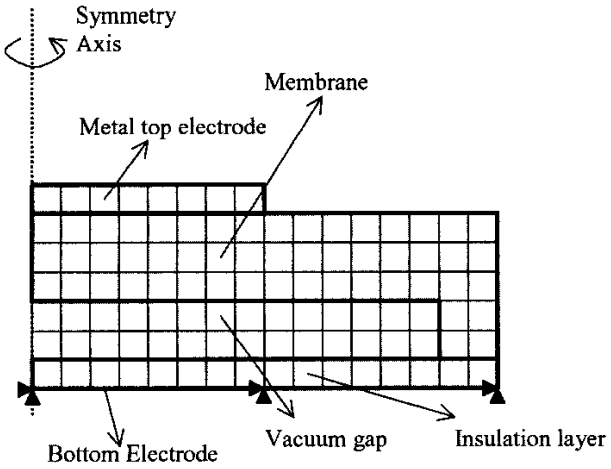

Fig. 4. FEM mesh of a CMUT membrane. The membrane material is silicon nitride (Young's modulus of 320 GPa, Poisson's ratio of 0.263, relative dielectric constant of 5.7 are used in the calculations). Black arrowheads on the bottom surface show the zero displacement boundary conditions on this surface. $d_m = 1$ μm, $d_0 = 0.3$ μm, radius = 50 μm, $d_i = 0$. Aluminum electrode thickness is 0.1 μm.

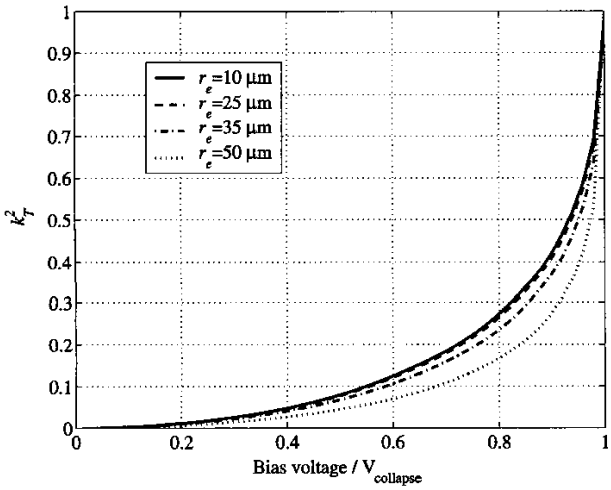

Fig. 5. Calculated coupling coefficient of the CMUT membrane for different electrode sizes.

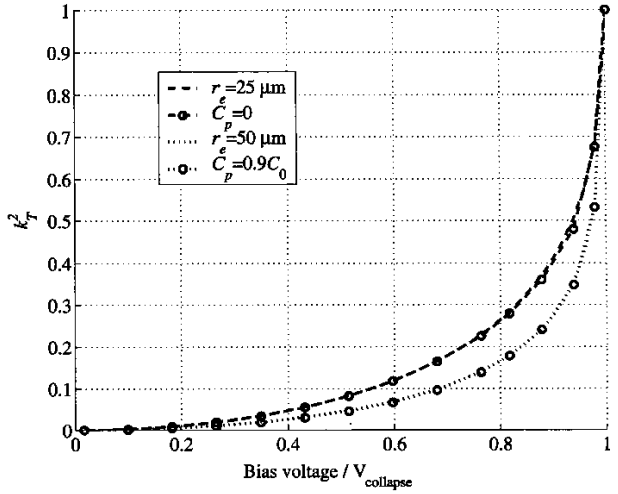

Fig. 6. Parallel plate approximation for a CMUT membrane. Curves with circles are obtained by adding parasitics to the parallel plate calculation.

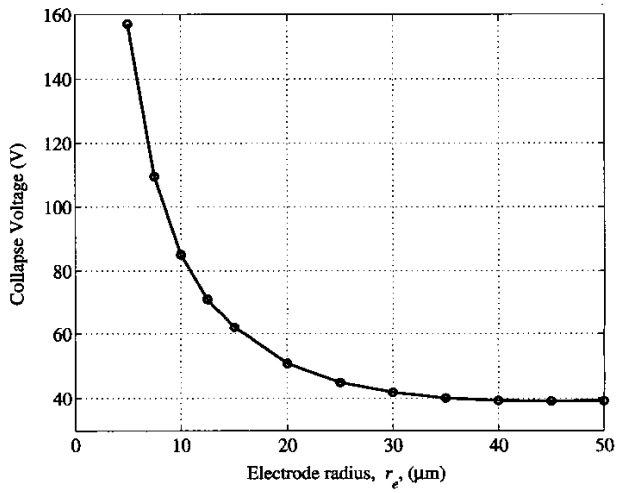

Fig. 7. Calculated collapse voltage as a function of electrode radius.

brane center and deflection reduces close to the rim. Therefore, the rate of increase of the free capacitance decreases as the electrode radius increases beyond half of the membrane radius.

The coupling coefficient of a membrane when the electrode radius is less than half of the membrane radius can be well approximated using the parallel plate assumption. This is due to the fact that, for small electrodes, the capacitance is located at the center of the membrane and changes as a parallel plate with the membrane moves. The k_T^2 curves for a CMUT membrane and a parallel plate capacitor are depicted in Fig. 6. For a larger electrode radius, the parallel parasitics of the membrane increases. The curve for a fully metalized membrane can be approximated by the coupling coefficient of a parallel plate capacitor with the appropriate amount of parasitics added as depicted in Fig. 6.

Note that, when electrode size increases, the collapse voltage decreases (Fig. 7). The decrease for small electrode sizes is more significant than for bigger electrodes. However, when the electrode radius is as large as one-half of the membrane radius, a further increase in the electrode size does not decrease the collapse voltage considerably. Therefore, both in terms of low collapse voltage and high coupling efficiency, half electrode coverage is the optimum structure. This result matches well with the optimum geometry suggested by Bozkurt *et al.* [11]. In this study, it has been shown that half electrode coverage reduces the parallel parasitic capacitances and, therefore, increases the transducer bandwidth.

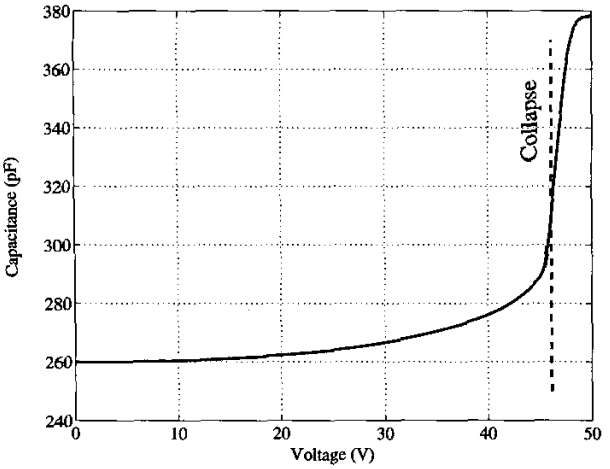

Fig. 8. Measured capacitance of the CMUT as a function of voltage.

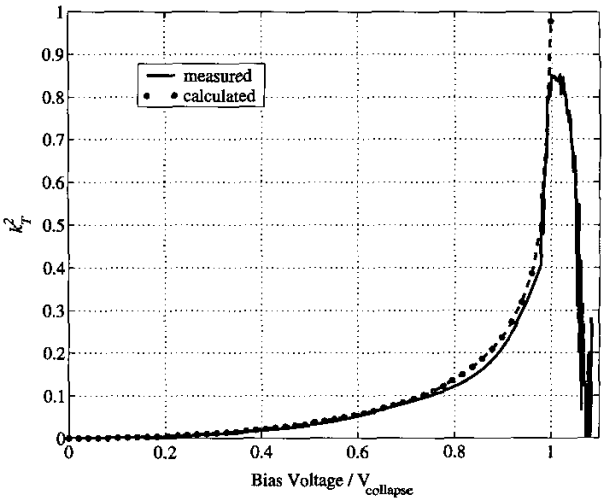

Fig. 9. The coupling coefficient obtained by using the capacitance curve shown in Fig. 8. The calculated curve is obtained with $C_p = 1.2C_0$. ($d_m = 0.85$ μm, $d_0 = 0.9$ μm, radius = 55 μm, $d_i = 0.16$ μm, $r_e = 30$ μm. Aluminum electrode thickness is 0.3 μm.)

III. Experimental Results

To validate the predictive power of the results obtained in the theory part of this paper, k_T^2 values were measured on real devices. The obtained values then were compared to the theoretical estimates. We measured the coupling coefficient of a CMUT fabricated for immersion applications. The total transducer area was 7 mm by 7 mm, and it was composed of more than 4900 membranes. The membrane thickness was 0.85 μm, the gap height was 0.9 μm, and the insulator layer thickness was 0.16 μm. The radii of the membrane and the electrode were 55 μm and 30 μm, respectively. The aluminum electrode was 0.3 μm thick, and the membrane was made of silicon nitride.

The coupling coefficient was determined by using (8). The measurements were performed in vacuum. The CMUT resonated below 1.5 MHz. Therefore, the fixed capacitance was measured using a network analyzer (HP8751A, Hewlett-Packard, Palo Alto, CA) in a frequency band of 4 MHz to 5 MHz, well above the resonance frequency. Higher order resonances were not observed in and around this frequency band. The measured capacitance is depicted in Fig. 8. For zero bias, the expected device capacitance was 120 pF. The remaining capacitance was due to the aluminum electrode off the membrane and the connectors between the network analyzer and the printed circuit board on which the transducer is attached. Therefore, the parallel parasitics for our measurement setup was 120%. The jump around 47 V reveals the collapse voltage. One might expect a more sudden jump at the collapse; however, the device is composed of many membranes. Collapse voltages of the individual membranes might be slightly different due to the small changes in the membrane dimensions over a large area. This results in a more smooth transition into collapse of the overall transducer. The collapse voltage depicted in Fig. 8 is determined by using the coupling coefficient calculation. The voltage with the highest k_T^2 is taken to be the collapse voltage. The free capacitance was calculated using (7). To reduce the noise on the calculation, a polynomial was fitted to the measured capacitance and the derivative was calculated by using the fitted curve. The measured and calculated coupling coefficients are depicted in Fig. 9. The maximum measured k_T^2 is 0.85. Close to collapse, it was difficult to determine the capacitance because even small AC signals could easily collapse the membranes, degrading the measurement accuracy.

An alternative method to measure coupling coefficient uses resonance (f_Y) and antiresonance (f_R) frequencies. The coupling coefficient then is defined by the following relation [5, p. 140]:

$$k_T^2 = 1 - \left(\frac{f_Y}{f_R}\right)^2. \tag{9}$$

Resonance frequencies can be determined by measuring the imaginary part of the impedance. As an example, Fig. 10 shows the measured impedance when the CMUT was biased at 39 V. The resonance and antiresonance frequencies were 1.253 and 1.412 MHz, respectively. Therefore, the k_T^2 is calculated to be 0.21. To get the complete k_T^2 curve, the bias voltage was swept from zero to 47 V. The resulting graph is depicted in Fig. 11. The FEM calculated k_T^2 and the calculated curve from capacitance measurement also are added to Fig. 11 for comparison purposes. Close to the collapse voltage, it was not possible to determine the resonance frequencies as the membranes collapsed easily even for very small AC signals. The problem is more prominent for resonance measurement than capacitance measurement because around the resonance the membrane can be set into large amplitude oscillations easily. This collapses the membrane. Both measurement methods, however, gave the same values for k_T^2 for voltages less than collapse voltage.

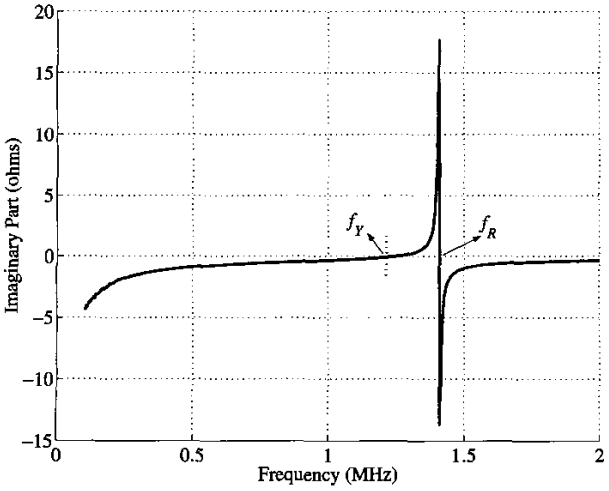

Fig. 10. Measured imaginary part of the input impedance of the CMUT.

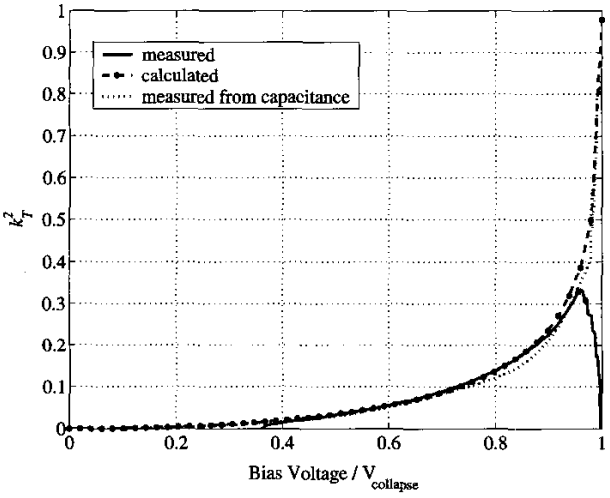

Fig. 11. Coupling coefficient by using resonance frequency measurement method. The calculated and measured curves in Fig. 9 also are added for comparison purposes.

IV. Conclusions

We have demonstrated the calculation and measurement of the coupling coefficient for CMUT membranes. Our FEM calculations showed that the coupling coefficient goes to unity regardless of the series and the parasitic capacitances at the collapse. For a given normalized bias voltage, the maximum coupling coefficient is achieved when the membrane is moved like a piston transducer. Therefore, the optimum geometry for a CMUT membrane is achieved when the electrode covers half of the membrane radius. This geometry minimizes the effect of the parallel parasitic inherent to the membrane. As the electrode radius is increased, the parallel parasitic increases, reducing the k_T^2. External parallel capacitances due to, for example, connections between the electronics and the transducer induce a similar effect. Although the half radius coverage is optimal, this increases the collapse voltage, and thus, increases the bias voltage. However, this is not a critical problem because the collapse voltage does not increase significantly when the electrode radius is as large as the half of the membrane radius.

The series parasitic capacitance modifies the effective gap height; therefore, the membrane displacement at the collapse increases. Thus, by carefully adjusting the series capacitance, it is possible to build devices without collapse. At collapse, the membrane simply makes contact with the bottom surface.

Our measurements validated the FEM calculations. According to the measurements, it is possible to bias the CMUT close to the collapse voltage to obtain high values of coupling coefficient ($k_T^2 = 0.85$). Close to collapse, it was difficult to measure the capacitance and resonance frequencies of the device as we performed experiments in a vacuum environment. However, when the device is immersed in a liquid and the membrane resonance will be heavily damped, one can expect to be able to measure higher coupling coefficients at voltages closer to the collapse voltage.

As a final note, the coupling coefficient has a direct impact on the device bandwidth for piezoelectric transducers. However, this is not the case for CMUTs. The bandwidth and k_T^2 relation is our current research topic.

Appendix A

In this Appendix, we will show the detailed derivations for spring softening, collapse voltage, and coupling coefficient calculations by assuming a parallel plate capacitor. Referring to Fig. 1, the capacitance of a parallel plate capacitor is given by:

$$C(x) = \frac{A\varepsilon_0}{\frac{d_i+d_m}{\varepsilon_r} + d_0 - x}, \tag{A1}$$

or

$$C(x) = \frac{A\varepsilon_0}{d_{\text{eff}} - x}, \tag{A2}$$

where A is the area, ε_0 is the permittivity of vacuum, and ε_r is the relative permittivity of the insulator and the membrane material; d_0 is the initial gap distance under zero bias voltage; d_i and d_m are the insulator and the membrane thickness, respectively. The electrostatic force applied on the top plate by the bottom plate is:

$$F_E = \frac{1}{2}QE, \tag{A3}$$

where $1/2E$ is the electric field due to the charge on the bottom plate. We also assumed that $+Q$ and $-Q$ are the charges on the top and bottom plates, respectively. Be-

cause Q is determined by the multiplication of the capacitance and the applied voltage, the electrostatic force is:

$$F_E = \frac{1}{2}\frac{C(x)}{d_{\text{eff}} - x}V^2, \tag{A4}$$

at a given bias voltage. The total net force on the top plate is given by:

$$F_N = \frac{1}{2}\frac{C(x)}{d_{\text{eff}} - x}V^2 - k_s x, \tag{A5}$$

where the second term in the right-hand side of the equation is the mechanical force. At the equilibrium, electrical attraction forces and mechanical restoring forces are equal to each other, and the resulting F_N is zero. Therefore, the relation between the applied voltage and the displacement is given by:

$$V = \sqrt{\frac{2k_s x}{A\varepsilon_0}}\,(d_{\text{eff}} - x), \tag{A6}$$

where k_s is the spring constant of the moving electrode. From (A3) one can calculate:

$$\frac{\mathrm{d}V}{\mathrm{d}x} = \sqrt{\frac{k_s}{2A\varepsilon_0 x}}\,(d_{\text{eff}} - 3x). \tag{A7}$$

Using (A5), the small signal spring constant of the system at a given bias voltage is:

$$\begin{aligned} k_s' &= \frac{\mathrm{d}}{\mathrm{d}x}F_N = -\frac{1}{2}\frac{\mathrm{d}}{\mathrm{d}x}\left(\frac{C(x)}{d_{\text{eff}} - x}\right)V^2 + k_s \\ &= -\frac{A\varepsilon_0 V^2}{(d_{\text{eff}} - x)^3} + k_s. \end{aligned} \tag{A8}$$

Note that, while calculating the small signal spring constant, the voltage should be assumed to be constant, because the main interest is the force gradient due to a small perturbation in the displacement. If (A8) is further manipulated, the small signal spring constant is given by:

$$k_s' = k_s\left(1 - \frac{2x}{d_{\text{eff}} - x}\right). \tag{A9}$$

Also note that, according to Hunt [5, p. 181], the softened spring constant is given by:

$$k_s' = k_s\left(1 - k_T^2\right), \tag{A10}$$

which is same as (A9).

The collapse occurs when the gradient of the total force F_N is negative. At that point, incremental increase in electrostatic force overcomes the incremental increase in the mechanical force. By equating (A8) to zero, it is found that the displacement is one-third of the effective gap at the collapse voltage:

$$x = \frac{d_{\text{eff}}}{3}, \tag{A11}$$

and the collapse voltage is given by:

$$V_{\text{col}} = \sqrt{\frac{8k_s d_{\text{eff}}^3}{27A\varepsilon_0}}. \tag{A12}$$

Small signal electrical and mechanical energies can be calculated as follows:

$$E_{\text{elec}} = \frac{1}{2}\left(C_p + C(x)\right)\mathrm{d}V^2, \tag{A13}$$

and

$$E_{\text{mech}} = \frac{1}{2}k_s'\mathrm{d}x^2. \tag{A14}$$

Note that above energy calculations are only valid at very low frequencies. The inertia of the membrane is not considered. If (A13) and (A14) are substituted in (1), one gets the coupling coefficient as:

$$k_T^2 = \frac{1}{1 + \frac{(C_p + C(x))}{k_s'}\left(\frac{\mathrm{d}V}{\mathrm{d}x}\right)^2}, \tag{A15}$$

where C_p is the parallel parasitics. The final equation for k_T^2 is:

$$k_T^2 = \frac{2x}{d_{\text{eff}} - x + (d_{\text{eff}} - 3x)\frac{C_p}{C(x)}}. \tag{A16}$$

Coupling coefficient also can be calculated analytically for parallel plate capacitors using Fraser's method. Fixed and free capacitances are given by:

$$C^S = \frac{\varepsilon_0 A}{d_{\text{eff}} - x} + C_p, \tag{A17}$$

$$C^T = \frac{\varepsilon_0 A}{d_{\text{eff}} - 3x} + C_p. \tag{A18}$$

If (A17) and (A18) are used in (8), the coupling coefficient of (A16) is obtained.

REFERENCES

[1] M. I. Haller and B. T. Khuri-Yakub, "A surface micromachined electrostatic ultrasonic air transducer," *IEEE Trans. Ultrason., Ferroelect., Freq. Contr.*, vol. 43, pp. 1–6, Jan. 1996.

[2] H. T. Soh, I. Ladabaum, A. Atalar, C. F. Quate, and B. T. Khuri-Yakub, "Silicon micromachined ultrasonic immersion transducers," *Appl. Phys. Lett.*, vol. 69, pp. 3674–3676, Dec. 1996.

[3] I. Ladabaum, X. Jin, H. T. Soh, A. Atalar, and B. T. Khuri-Yakub, "Surface micromachined capacitive ultrasonic transducers," *IEEE Trans. Ultrason., Ferroelect., Freq. Contr.*, vol. 45, pp. 678–690, May 1998.

[4] G. S. Kino, *Acoustic Waves: Devices, Imaging, and Signal Processing.* Englewood Cliffs, NJ: Prentice-Hall, 1987.

[5] F. V. Hunt, *Electroacoustics; The Analysis of Transduction, and Its Historical Background.* Cambridge, MA: Harvard Univ. Press, 1954.

[6] S. D. Senturia, *Microsystem Design.* Boston: Kluwer Academic Pub., 2001.

[7] P.-C. Eccardt, K. Niederer, and B. Fischer, "Micromachined transducers for ultrasound applications," in *Proc. IEEE Ultrason. Symp.*, 1997, pp. 1609–1618.

[8] E. K. Chan and R. W. Dutton, "Electrostatic micromechanical actuator with extended range of travel," *J. Microelectromech. Syst.*, vol. 9, no. 3, pp. 321–328, Sep. 2000.

[9] J. Fraser and P. Reynolds, "Finite-element method for determination of electromechanical coupling coefficient for piezoelectric and capacitive micromachined ultrasonic transducers," presented at Joint 140th meeting of ASA/NOISE-CON, 2000.

[10] D. Berlincourt, "Piczoelectric crystals and ceramics," in *Ultrasonic Transducer Materials*. O. E. Mattiat, Ed. New York: Plenum, 1971.

[11] A. Bozkurt, I. Ladabaum, A. Atalar, and B. T. Khuri-Yakub, "Theory and analysis of electrode size optimization for capacitive microfabricated ultrasonic transducers," *IEEE Trans. Ultrason., Ferroelect., Freq. Contr.*, vol. 46, pp. 1364–1374, Nov. 1999.

Goksen Goksenin Yaralioglu (S'92, M'99) was born in Akhisar, Turkey, on May 13, 1970. He received his B.S., M.S., and Ph.D. degrees from Bilkent University, Ankara, Turkey, in 1992, 1994, and 1999, respectively, all in electrical engineering.

He is now working as an engineering research associate in E. L. Ginzton Laboratory, Stanford University, Stanford, CA. His current research interests include design, modeling, and applications of micromachined ultrasonic transducers, and atomic force microscopy at ultrasonic frequencies.

Arif Sanli Ergun (S'91, M'99) was born in Ankara, Turkey, in 1969. He received his B.Sc., M.Sc., and Ph.D. degrees in 1991, 1994, and 1999, respectively, all in electrical and electronics engineering from Bilkent University, Ankara, Turkey.

He is now in E. L. Ginzton Laboratory, Stanford University, Stanford, CA, as an engineering research associate. His main research interests are acoustics, ultrasound, microelectromechanical systems (MEMS), and microwave electronics.

Baris Bayram was born in Izmir, Turkey. He received the B.S. degree in 2000 from Bilkent University, Ankara, Turkey, the M.S. degree in 2002 from Stanford University, Stanford, CA, both in electrical engineering. He is currently a Ph.D. candidate at the E. L. Ginzton Laboratory, Stanford University. His current research interests include the modelling, simulation, fabrication, and experimental characterization of capacitive micromachined ultrasonic transducers for low voltage and reduced crosstalk operation.

Edward Hæggström is a visiting scholar at Ginzton Lab (Khuri-Yakub group), Stanford University, Stanford, CA, on leave from his position as assistant professor at the Department of Physics at the University of Helsinki, Finland. He received his D.Sc. degree in 1998 in applied physics from the University of Helsinki, Finland, and a M.B.A. in innovation management from the Helsinki University of Technology in 2001.

His principal research interests are within ultrasonic characterization of biological samples.

Butrus T. Khuri-Yakub (S'70–S'73–M'76–SM'87–F'95) was born in Beirut, Lebanon. He received the B.S. degree in 1970 from the American University of Beirut, the M.S. degree in 1972 from Dartmouth College, Hanover, NH, and the Ph.D. degree in 1975 from Stanford University, Stanford, CA, all in electrical engineering.

He joined the research staff at the E. L. Ginzton Laboratory of Stanford University in 1976 as a research associate. He was promoted to a senior research associate in 1978, and to a professor of electrical engineering (research) in 1982. He has served on many university committees in the School of Engineering and the Department of Electrical Engineering.

He currently is the Deputy Director of the E. L. Ginzton Laboratory. Professor Khuri-Yakub has been teaching at both the graduate and undergraduate levels for more than 15 years, and his current research interests include in situ acoustic sensors (temperature, film thickness, resist cure, etc.) for monitoring and control of integrated circuits manufacturing processes, micromachining silicon to make acoustic materials and devices such as airborne and water immersion ultrasonic transducers and arrays, and fluid ejectors, and in the field of ultrasonic nondestructive evaluation and acoustic imaging and microscopy.

Professor Khuri-Yakub is a fellow of the IEEE, a senior member of the Acoustical Society of America, and a member of Tau Beta Pi. He is associate editor of *Research in Nondestructive Evaluation*, a journal of the American Society for Nondestructive Testing. Professor Khuri-Yakub has authored more than 300 publications and has been principle inventor or co-inventor of 52 issued patents. He received the Stanford University School of Engineering Distinguished Advisor Award, June 1987, and the Medal of the City of Bordeaux for contributions to nondestructive evaluation, 1983.